

# Generalized method for finding community structures in networks

Chang Chang<sup>1, 2\*</sup>

<sup>1</sup>School of Life Sciences, Peking University, Beijing 100871, China

<sup>2</sup>Center for Quantitative Biology, Peking University, Beijing 100871, China

\*chang.connected@pku.edu.cn

PACS number(s): 89.75.Hc, 02.10.Ox, 02.50.-r, 87.18.Vf

Version: arXiv:1307.7569, version 2

Date: Nov 6, 2013

## Abstract

To date, most algorithms aiming to find community structures focus on unipartite or bipartite networks. As is known, a unipartite network consists of one set of nodes, and a bipartite network consists of two sets of nonoverlapping nodes with links only join nodes in different sets. However, a third type exists, defined as the *mixture network* in our paper. Just like a bipartite network, a mixture network also consists of two sets of nodes, but some nodes may simultaneously belong to two sets, which breaks the nonoverlapping restriction of a bipartite network. The mixture network can be considered as a general case, with unipartite and bipartite networks viewed as its limiting cases. A mixture network can represent not only all the unipartite and bipartite networks but also a wide range of real-world networks that cannot be properly represented as unipartite or bipartite networks in fields including biology and social science. Based on this observation, we first propose a probabilistic model that can find modules in unipartite, bipartite, and mixture networks in a unified framework based on the link community model for a unipartite, undirected network [B. Ball, B. Karrer, and M. E. J. Newman, Phys. Rev. E **84**, 036103 (2011)]. We test our algorithm on synthetic networks (both overlapping and non-overlapping communities) and apply it to two real-world networks, southern women bipartite network and a human transcriptional regulatory mixture network. The results suggest that our model performs well on all three types of networks, is competitive with other algorithms for unipartite and bipartite networks, and is applicable to real-world networks.

## I. INTRODUCTION

Community structure, or network modules, has become a fruitful topic in fields such as physics, mathematics, biology, and social science [1]. To date, most algorithms focusing on this problem operate on either unipartite [2-7] or bipartite networks [8-10], and some deal with both [11, 12] (reviewed in [1, 13]). A unipartite network consists of a vertex set and an edge set joining pairs of vertices. On the other hand, a bipartite network consists of two disjoint sets of vertices and a set of edges such that each edge only joins vertices in different sets. Most complex networks in nature and society are represented either as unipartite or as bipartite [1].

However, a third type of network also exists, defined as the *mixture network* in our paper. Just like a bipartite network, a mixture network also consists of two sets of nodes, but some nodes may simultaneously belong to two sets rather than one, which breaks the nonoverlapping restriction. When all nodes belong to two sets, a mixture network is unipartite; when each node only belongs to one of the two sets, it is bipartite; when only a part of nodes belong to two sets, it is neither unipartite nor bipartite. Thus the mixture network can be considered as a general case, with unipartite and bipartite networks viewed as its limiting cases. A mixture network can represent not only all the unipartite and bipartite networks but also a wide range of real-world networks that cannot be properly represented as unipartite or bipartite networks in fields including biology and social science (For the convenience of illustration, we will use mixture network only to denote the mixture networks that are neither unipartite nor bipartite hereafter):

(i) Transcriptional regulatory networks [14-16]: one vertex set represents transcriptional factors (TFs), which play the role of regulators, and another set represents a collection of downstream target genes. Since some TFs can also play the role of target genes, interactions can occur not only between a TF and a target gene but also between TFs [14], suggesting that certain TFs belong to both vertex sets simultaneously rather than only one. Considering the fact that most of the target genes do not play the role of regulators, edges exist between the two vertex sets that are

neither disjoint nor identical. Consequently, transcriptional regulatory networks are mixture networks rather than unipartite or bipartite networks.

(ii) Phosphorylation networks [17]: one vertex set consists of kinases or phosphatases, and another set consists of target proteins being phosphorylated or dephosphorylated. Some kinases or phosphatases can also be phosphorylated or dephosphorylated by other kinases or phosphatases, playing both roles in the network.

(iii) Shareholding networks [18]: one vertex set represents the owners and another set represents corporations or stocks. Since a corporation can also be owned by another corporation, and not all the owners are corporations, it makes shareholding networks examples of mixture networks.

(vi) Some genetic interaction networks built from epistatic mini-array profiles [19-22]: in such networks, one vertex set represents query genes, and the other set represents array genes. Two genes are linked if they have a genetic interaction. One gene can be either a query gene or an array gene, and sometimes it can be both. Ideally, the case of measuring genetic interactions between all pairs of genes would lead to a unipartite network [23, 24]. However, these result in mixture networks because of the research goal or funding limitation in many studies like Refs. [19-21] or epistatic mini-array profiles focusing on the cell cycle of *Saccharomyces cerevisiae* and *Schizosaccharomyces pombe* conducted by our group [22], so that only interactions between two subsets of genes that share common genes are measured.

(v) Some protein interaction networks built by the yeast two-hybrid method [25]: one vertex set represents bait proteins and another set represents prey proteins. The reason for network of Ref. [25] being a mixture network is due to the experimental design.

The above examples can be summarized into two types of mixture networks. The first type consists two vertex sets of two roles, some nodes of which can play both roles, thus they simultaneously belong to two sets rather than one. On the other hand, the second type is a subset of a corresponding unipartite network, since only links between two subsets of nodes that share certain common elements are known. All

examples mentioned above belong to the first type, and examples (iv-v) also belong to the second type.

In past studies, different approaches have been used to analyze mixture networks, although the concept is not explicitly formed. However, many suffer drawbacks when used for mixture networks without considering their own characteristics. To begin with, directly using algorithms that can work for bipartite networks, such as biclustering [26] or hierarchical clustering [20], will omit the association between pairs of nodes that are actually one. Such nodes may be partitioned into different modules improperly even when a community detection algorithm does not allow overlapping community, or be assigned to the same module with two different weights or probabilities. Besides, projecting a mixture network to unipartite is an alternative choice [21], but information will be lost in such a process just as that for a bipartite network [8, 27], and only one vertex set, rather than both, can be assigned to modules after the transformation. Furthermore, imputation methods can be used to convert the second type of mixture networks to unipartite ones by predicting missing values [28], but the performance of a community detection algorithm will then depend on the performance of an imputation method been used. Thus, models specific for mixture networks are necessary.

We set out to find network modules in unipartite, bipartite and mixture networks in a unified frame, allowing the relationship between two vertex sets be identical, disjointed, or neither. To achieve this goal, we propose a probabilistic method that operates on all three types of network based on the link community model for unipartite networks developed by Ball *et al.* [6] (denoted as BKN hereafter).

This paper is organized as follows. To begin with, we review BKN for a unipartite, undirected network in Sec. IIA, and redefine this model in the context of a bipartite network and generalize it to a mixture network (the general case) in the remaining subsections of Sec. II. In Sec. III and IV, we explore the performance of the model on synthetic networks generated using the model itself and those generated by sampling, two ways of generating all three types of networks. In Sec. V and VI, we apply the model to random unipartite, directed networks and bipartite networks.

Subsequently, we apply the model on real-world data of bipartite and mixture networks in Sec. VII. Note that simulations and applications for real-world data solely for unipartite, undirected networks is not needed to be discussed in this paper, since they have been done by Ref. [6]. In Sec. VIII, we provide a discussion.

## II. GENERATIVE MODELS FOR MODULE DETECTION

### A. Unipartite network

Since our model is an extension and generalization of BKN, we briefly review this generative model for unipartite, undirected networks in this subsection.

Let  $G_U = (V, E)$  denote an unipartite, undirected network, where  $V$  is the vertex set and  $E$  is the edge set.  $\mathbf{A}$  represents the adjacency matrix, where  $A_{ij} = 1$  if there is a link between vertex  $i$  and vertex  $j$ , and  $A_{ii} = 2$  if there is a self-loop of vertex  $i$ . Suppose the number of modules  $K$  is given. BKN is parameterized by a set of parameters  $\theta$ , such that  $\theta_{iz}$  represents the propensity of vertex  $i$  to belong to module  $z$ . Specifically, the physical meaning of  $\theta_{iz}\theta_{jz}$  is the expected number of links between vertex  $i$  and vertex  $j$  belonging to module  $z$ , with the exact number being Poisson-distributed. By summing over all  $K$  modules,  $\sum_z \theta_{iz}\theta_{jz}$  represents the expected number between vertex  $i$  and vertex  $j$ , the exact number of which is also Poisson-distributed, since the sum of independent Poisson variables is still Poisson-distributed. Given that the actual number of edges between  $i$  and  $j$  is known, the likelihood function of the unipartite, undirected network  $G_U$  with the adjacency matrix  $\mathbf{A}$  is

$$\begin{aligned}
 P(G_U | \theta) = & \prod_{i < j} \frac{\left(\sum_z \theta_{iz}\theta_{jz}\right)^{A_{ij}}}{A_{ij}!} \exp\left(-\sum_z \theta_{iz}\theta_{jz}\right) \\
 & \times \prod_i \frac{\left(\frac{1}{2}\sum_z \theta_{iz}\theta_{iz}\right)^{A_{ii}/2}}{(A_{ii}/2)!} \exp\left(-\frac{1}{2}\sum_z \theta_{iz}\theta_{iz}\right).
 \end{aligned} \tag{1}$$

BKN can be fitted to an observed network according to the maximum likelihood

principle with respect to parameters  $\theta_{iz}$ . By taking the logarithm of Eq. (1) and discarding constant terms, the log likelihood function of the model can be written as

$$\ln P(G_U | \theta) = \sum_{ij} A_{ij} \ln \left( \sum_z \theta_{iz} \theta_{jz} \right) - \sum_{ijz} \theta_{iz} \theta_{jz}. \quad (2)$$

Applying Jensen's inequality, we obtain

$$\ln P(G_U | \theta) \geq \sum_{ijz} \left[ A_{ij} q_{ij}(z) \ln \left( \frac{\theta_{iz} \theta_{jz}}{q_{ij}(z)} \right) - \theta_{iz} \theta_{jz} \right] \quad (3)$$

by introducing an arbitrary variable  $q_{ij}(z)$ , which satisfies  $\sum_z q_{ij}(z) = 1$ . When

$$q_{ij}(z) = \frac{\theta_{iz} \theta_{jz}}{\sum_z \theta_{iz} \theta_{jz}}, \quad (4)$$

the inequality becomes an exact equality. By differentiating Eq. (3) with respect to  $\theta_{iz}$ , we obtain

$$\theta_{iz} = \frac{\sum_j A_{ij} q_{ij}(z)}{\sum_j \theta_{jz}}, \quad (5)$$

which gives the optimal value of  $\theta_{iz}$ . In Ref. [6], Ball *et al.* further change the form of Eq. (5) to

$$\theta_{iz} = \frac{\sum_j A_{ij} q_{ij}(z)}{\sqrt{\sum_{ij} A_{ij} q_{ij}(z)}}, \quad (6)$$

using the fact that  $\sum_i \theta_{iz} = \sum_j \theta_{jz}$ .

BKN is an expectation–maximization (EM) algorithm, which can be used to find the maximum likelihood in an iterative manner. The log likelihood increases monotonically by updating the parameters iteratively using Eqs. (4) and (5) or Eqs. (4) and (6), which can be viewed as two variants of EM, the former known as the expectation conditional maximization (ECM) [29], and the latter as an incremental variant of the EM [30]. Multiple random initializations are needed to escape from local maxima and the division with the highest log likelihood is chosen as the final result.

Since the physical meaning of  $q_{ij}(z)$  is the weight of the edge between vertex  $i$

and vertex  $j$  belonging to module  $z$ , this quantity is used to infer link communities in the network. Mathematically, vertex  $i$  belongs to module  $z$  if  $\sum_j A_{ij} q_{ij}(z) \geq 1$  [31], and the physical meaning of the left-hand side of this inequality is the average number of links belonging to module  $z$  that link to vertex  $i$ .

## B. Bipartite network

In this subsection, we redefine BKN in the context of a bipartite network. In a unipartite network, all links exist within the same group of vertices. Consequently, one set of parameters,  $\theta$ , is enough to describe the underlying structure of unipartite networks. On the other hand, there is two set of vertices in a bipartite network, thus two set of parameters should be used for the parameterization. Given a bipartite network  $G_B = (U, V, E)$ , where  $U$  and  $V$  denote two disjoint vertex sets, and  $E$  denotes the edge set. We use two sets of parameters  $\theta^{(U)}$  and  $\theta^{(V)}$  to describe the underlying structure of a bipartite network, such that  $\theta_{iz}^{(U)}$  represents the propensity of vertex  $i$  in the vertices of set  $U$  belonging to module  $z$ , and  $\theta_{jz}^{(V)}$  represents the propensity of vertex  $j$  in the vertices of set  $V$  belonging to module  $z$ . Similar to BKN, the physical meaning of  $\theta_{iz}^{(U)} \theta_{jz}^{(V)}$  is the expected number of links between vertex  $i$  in vertex set  $U$  and vertex  $j$  in vertex set  $V$  belonging to module  $z$ , with the exact number being Poisson-distributed. By summing over all  $K$  modules,  $\sum_z \theta_{iz}^{(U)} \theta_{jz}^{(V)}$  represents the expected number of links between vertex  $i$  in vertex set  $U$  and vertex  $j$  in vertex set  $V$ , the exact number of which is still Poisson-distributed. The likelihood function of generating a bipartite network  $G_B$  is

$$P(G_B | \theta^{(U)}, \theta^{(V)}) = \prod_{ij} \frac{(\sum_z \theta_{iz}^{(U)} \theta_{jz}^{(V)})^{A_{ij}}}{A_{ij}!} \exp\left(-\sum_z \theta_{iz}^{(U)} \theta_{jz}^{(V)}\right). \quad (7)$$

By taking the logarithm of the likelihood function, and applying Jensen's inequality with an arbitrary variable  $q_{ij}(z)$  that satisfies  $\sum_z q_{ij}(z) = 1$  be introduced, we get

$$\ln P(G_B | \theta^{(U)}, \theta^{(V)}) \geq \sum_{ijz} \left[ A_{ij} q_{ij}(z) \ln \left( \frac{\theta_{iz}^{(U)} \theta_{jz}^{(V)}}{q_{ij}(z)} \right) - \theta_{iz}^{(U)} \theta_{jz}^{(V)} \right], \quad (8)$$



where the optimal value of  $q_{ij}(z)$  is given by

$$q_{ij}(z) = \frac{\theta_{iz}^{(U)} \theta_{jz}^{(V)}}{\sum_z \theta_{iz}^{(U)} \theta_{jz}^{(V)}}, \quad (9)$$

with the physical meaning unchanged compared to that of BKN. The optimal values of  $\theta_{iz}^{(U)}$  and  $\theta_{jz}^{(V)}$  are given by

$$\theta_{iz}^{(U)} = \frac{\sum_j A_{ij} q_{ij}(z)}{\sum_j \theta_{jz}^{(V)}}, \quad \theta_{jz}^{(V)} = \frac{\sum_i A_{ij} q_{ij}(z)}{\sum_i \theta_{iz}^{(U)}}, \quad (10)$$

by differentiating Eq. (8) with respect to  $\theta_{iz}^{(U)}$  and  $\theta_{jz}^{(V)}$ . In statistics, this is known as ECM. The criterion that vertex  $i$  in  $U$  belongs to module  $z$  is  $\sum_j A_{ij} q_{ij}(z) \geq 1$  and that of vertex  $j$  in  $V$  belongs to module  $z$  is  $\sum_i A_{ij} q_{ij}(z) \geq 1$ .

### C. The mixture network as an unified framework

As noted, the mixture network can be considered as a general case, with the unipartite and bipartite networks as limiting cases. As a consequence, we can define the generative model in a unified framework.

Given a graph  $G = (U, V, E)$ , where  $U$  and  $V$  represent two sets of vertices, and  $E$  is the set of edges between vertices in  $U$  and  $V$ , the relationship between  $U$  and  $V$  determines the type of  $G$ , which can classify networks into three types: (1) Unipartite: when  $U$  and  $V$  are identical, all edges are within the same set of vertices, then  $G$  is unipartite. (2) Bipartite: when  $U$  and  $V$  are disjoint,  $G$  is bipartite, and each edge in  $E$  links nodes from two disjoint sets. (3) Mixture: when  $U$  and  $V$  are neither identical nor disjoint, i.e., they have some common vertices but not all vertices are same, it is a mixture network.

Vertex labels, or identifiers, are needed to determine whether a vertex is shared by two vertex sets. Let  $l_i^{(U)}$  denote the label of vertex  $i$  in  $U$ , and  $l_j^{(V)}$  denote the label of vertex  $j$  in  $V$ . In each set, any label is unique. When label for vertex  $i$  in  $U$  is the same as that of vertex  $j$  in  $V$ ,  $i$  and  $j$  are the same vertex rather than two different vertices. For simplicity, let  $O_U$  and  $O_V$  denote two sets of nodes in  $U$  and  $V$  that

share common labels (common vertices), while  $S_U$  and  $S_V$  denote two sets of vertices in  $U$  and  $V$  that do not share any common label (specific vertices).

An illustration of the relationship between the mixture network and the unipartite network and the mixture network is given in Fig. 1.

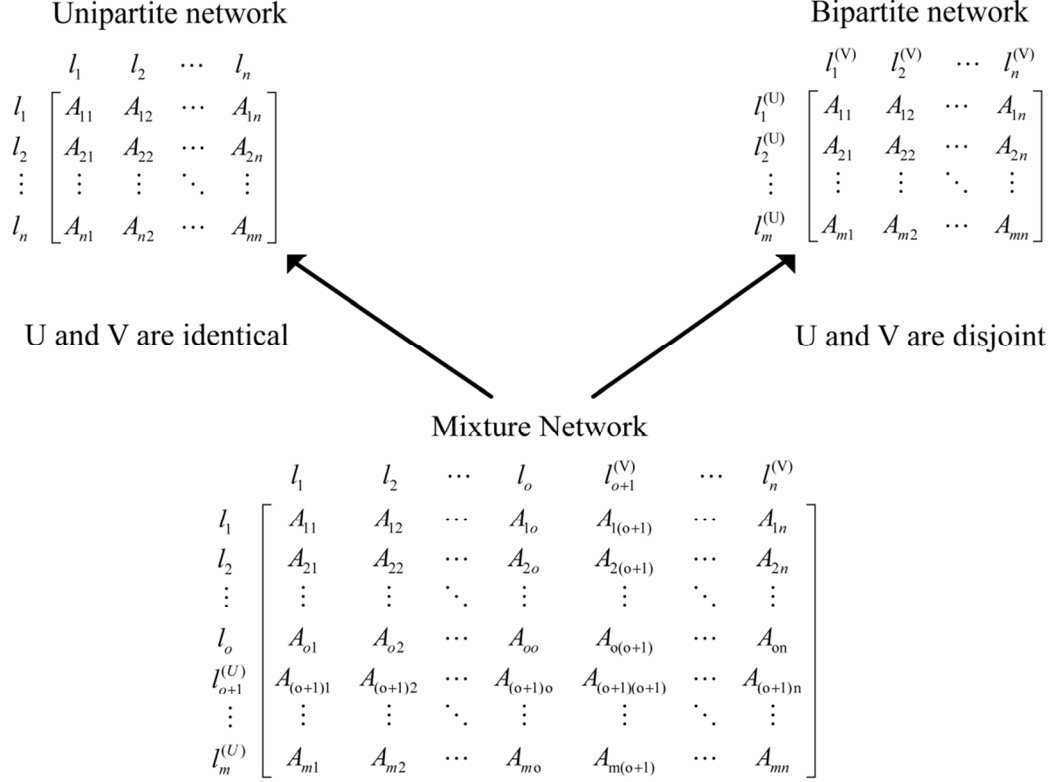


FIG 1. The mixture network can be considered as a general case. The elements of adjacency matrices are enclosed in square bracket and the labels of vertices are placed at the left or the top. For convenience of illustration, the adjacency matrix for the mixture network is rearranged so that the sub-matrix of all common vertices is at the left-up corner, and the labels for each pair in this sub-matrix at  $i$ th row and  $i$ th column both equal to  $l_i$ . For a mixture network, when  $U$  and  $V$  are identical, only the sub-matrix of all common vertices remain, which is the adjacency matrix for unipartite; on the other hand, when  $U$  and  $V$  are disjoint, only the sub-matrix of all specific vertices remain, which is the adjacency matrix for bipartite.

The generalization of the bipartite network version model to mixture network is based on a simple idea: if two vertices are actually the same one, it should only has

one underlying tendency. This is reached by constrained the tendencies of this pair of nodes to belong to the same module be the same. This idea is quite similar to that in the comment of Costa and Hensen [32], which suggest that a unipartite network can be transformed into a bipartite network by adding explicit constraints specifying that each pair of corresponding nodes must belong to the same community. Again, the tendency of vertex  $i$  in  $U$  and vertex  $j$  in  $V$  belonging to module  $z$  is denoted as  $\theta_{iz}^{(U)}$  and  $\theta_{jz}^{(V)}$ . Consequently, the likelihood function of the mixture networks is

$$P(G | \theta^{(U)}, \theta^{(V)}) = \prod_{ij} \frac{(\sum_z \theta_{iz}^{(U)} \theta_{jz}^{(V)})^{A_{ij}}}{A_{ij}!} \exp\left(-\sum_z \theta_{iz}^{(U)} \theta_{jz}^{(V)}\right), \quad (11)$$

subject to constraints that

$$\delta_{i^{(U)}, j^{(V)}} (\theta_{iz}^{(U)} - \theta_{jz}^{(V)}) = 0 \quad \forall i, j, z, \quad (12)$$

where  $\delta$  is the Kronecker delta function. Fundamentally speaking, a random network generated by this generative model is a directed network, since its unipartite part does not necessarily need to be symmetric [33]. For an undirected network, we adopt the view that an undirected edge can be viewed as two directed edges in opposite directions [34]. For self-loops, there exists a slightly difference comparing to that in BKN. Unlike other undirected edges, a self-loop only has one corresponding element in the adjacency matrix. Thus, when vertex  $i$  in  $U$  and vertex  $j$  in  $V$  are actually one node and they have a link (i.e., self-loop), the value of  $A_{ij}$  is 1 rather than 2 regardless whether the network is directed or undirected.

Such an optimization problem with equality constraints can be solved using the Lagrange multiplier. The proof is available at **Appendix A**.

We introduce an arbitrary variable  $q_{ij}(z)$  that satisfies  $\sum_z q_{ij}(z) = 1$ . The optimal value of  $q_{ij}(z)$  is given by

$$q_{ij}(z) = \frac{\theta_{iz}^{(U)} \theta_{jz}^{(V)}}{\sum_z \theta_{iz}^{(U)} \theta_{jz}^{(V)}}. \quad (13)$$

For  $\theta_{iz}^{(U)}$  and  $\theta_{jz}^{(V)}$ , two conditions will be considered separately: (1) For any

pair of common vertices  $i'$  in  $O_U$  and  $j'$  in  $O_V$  that  $\delta_{i',j'}^{(U),j'(V)} = 1$ , we get

$$\theta_{iz}^{(U)} = \frac{\sum_i A_{ij'} q_{ij'}(z) + \sum_j A_{i'j} q_{i'j}(z)}{\sum_i \theta_{iz}^{(U)} + \sum_j \theta_{jz}^{(V)}}, \quad \theta_{jz}^{(V)} = \frac{\sum_i A_{ij'} q_{ij'}(z) + \sum_j A_{i'j} q_{i'j}(z)}{\sum_i \theta_{iz}^{(U)} + \sum_j \theta_{jz}^{(V)}}; \quad (14)$$

(2) For specific vertex  $i$  in  $S_U$  or  $j$  in  $S_V$ , we have

$$\theta_{iz}^{(U)} = \frac{\sum_j A_{ij} q_{ij}(z)}{\sum_j \theta_{jz}^{(V)}}, \quad \theta_{jz}^{(V)} = \frac{\sum_i A_{ij} q_{ij}(z)}{\sum_i \theta_{iz}^{(U)}}. \quad (15)$$

Our model for a mixture network is a general solution, since both BKN (unipartite, undirected network version) and the bipartite network version described in the preceding subsection can be described as limiting cases. When all vertices of  $U$  and  $V$  are common vertices (unipartite network), only Eq. (14) remains. Since the network that BKN studied is symmetric, we have  $\sum_i A_{ij'} q_{ij'}(z) = \sum_j A_{i'j} q_{i'j}(z)$  and  $\sum_i \theta_{iz}^{(U)} = \sum_j \theta_{jz}^{(V)}$ , Eq. (14) can be reduced to Eq. (5). When all vertices of  $U$  and  $V$  are specific vertices (bipartite network), only Eq. (15) remains, which is exactly the same as Eq. (10). On the other side, the form of equations for  $q_{ij}(z)$  remains constant for all three versions of the models.

In the general model, the criteria for a node belongs to a module depend on whether this node is a common or specific vertex and whether the network is directed or undirected. For a specific vertex, the criterion is same as that of the bipartite network version model: vertex  $i$  in  $S_U$  belongs to module  $z$  if  $\sum_j A_{ij} q_{ij}(z) \geq 1$ , and vertex  $j$  in  $S_V$  belongs to module  $z$  if  $\sum_i A_{ij} q_{ij}(z) \geq 1$ . For a common vertex, the criterion depends on whether the network is directed or undirected. When the network is undirected, the unipartite part of the network is symmetric. For a pair of corresponding common vertices  $i'$  and  $j'$ , we only need to count links between common vertices once, i.e.,  $\sum_{i \in S_U} A_{ij'} q_{ij'}(z) + \sum_j A_{i'j} q_{i'j}(z) \geq 1$ . When the network is directed, links between common vertices should be counted twice rather than once,

i.e.,  $\sum_i A_{ij} q_{ij}(z) + \sum_j A_{ij} q_{ij}(z) \geq 1$ . According to the criteria, a node can belong to one module, several modules, or none of the modules.

### III. SIMULATIONS OF CONSISTENCY TESTS

In this section, we perform several consistency tests, which test the algorithm in terms of the random networks generated from the generative model itself with different parameters.

#### A. Synthetic networks generated by the generative model

Using the generative model described in the previous section to generate random networks can be viewed as the reverse process of finding network modules using the same model. When aiming to find modules, we infer module structures from the adjacency matrix; on the other side, when the model is used to generate random networks, community structures are known and adjacency matrices are generated based on the the hidden variables of the model.

The process of generating a random mixture network is described as follows: (1) assign module membership to vertices; (2) set expected number of links for nodes to each module; (3) calculate parameters; (4) calculate expected number of links between each pair of nodes; and (5) generate the adjacency matrix. In this study, we generate adjacency matrices with binary elements by forcing its element to be 1 if it is larger than 1, despite that our model can deal with multiedge problem technically.

Let  $k_{iz}^{(U)} = \sum_j A_{ij} q_{ij}(z)$  and  $k_{jz}^{(V)} = \sum_i A_{ij} q_{ij}(z)$ , which are set by the user to denote the average number of links belonging to module  $z$  that links to vertex  $i$  in  $U$  and vertex  $j$  in  $V$ , respectively. The values of  $\sum_{i \in O_U} \theta_{iz}^{(U)}$ ,  $\sum_{i \in S_U} \theta_{iz}^{(U)}$ ,  $\sum_{j \in S_V} \theta_{jz}^{(V)}$ , and  $\sum_{j \in O_V} \theta_{jz}^{(V)}$  can be given by

$$\begin{aligned}
\sum_{i \in O_U} \theta_{iz}^{(U)} &= \sqrt{\frac{\left(\sum_{i \in O_U} k_{iz}^{(U)} + \sum_{j \in O_V} k_{jz}^{(V)}\right)^2 - \left(\sum_{i \in S_U} k_{iz}^{(U)} - \sum_{j \in S_V} k_{jz}^{(V)}\right)^2}{2\left(\sum_{i \in S_U} k_{iz}^{(U)} + \sum_{j \in S_V} k_{jz}^{(V)} + \sum_{i \in O_U} k_{iz}^{(U)} + \sum_{j \in O_V} k_{jz}^{(V)}\right)}}, \\
\sum_{i \in S_U} \theta_{iz}^{(U)} &= \frac{2\sum_{i \in S_U} k_{iz}^{(U)}}{\sum_{j \in S_V} k_{jz}^{(V)} - \sum_{i \in S_U} k_{iz}^{(U)} + \sum_{i \in O_U} k_{iz}^{(U)} + \sum_{j \in O_V} k_{jz}^{(V)}} \sum_{i \in O_U} \theta_{iz}^{(U)}, \\
\sum_{j \in S_V} \theta_{jz}^{(V)} &= \frac{2\sum_{j \in S_V} k_{jz}^{(V)}}{\sum_{i \in S_U} k_{iz}^{(U)} - \sum_{j \in S_V} k_{jz}^{(V)} + \sum_{i \in O_U} k_{iz}^{(U)} + \sum_{j \in O_V} k_{jz}^{(V)}} \sum_{i \in O_U} \theta_{iz}^{(U)}, \\
\sum_{j \in O_V} \theta_{jz}^{(V)} &= \sum_{i \in O_U} \theta_{iz}^{(U)}.
\end{aligned} \tag{16}$$

For common vertices  $i'$  in  $O_U$  and  $j'$  in  $O_V$  that  $\delta_{i',j'}^{(U),(V)} = 1$ ,

$$\begin{aligned}
\theta_{i'z}^{(U)} &= \sum_{i \in O_U} \theta_{iz}^{(U)} \frac{k_{i'z}^{(U)} + k_{j'z}^{(V)}}{\sum_{i \in O_U} k_{iz}^{(U)} + \sum_{j \in O_V} k_{jz}^{(V)}}, \\
\theta_{j'z}^{(V)} &= \sum_{j \in O_V} \theta_{jz}^{(V)} \frac{k_{i'z}^{(U)} + k_{j'z}^{(V)}}{\sum_{i \in O_U} k_{iz}^{(U)} + \sum_{j \in O_V} k_{jz}^{(V)}}.
\end{aligned} \tag{17}$$

For specific vertices  $i$  in  $S_U$  and  $j$  in  $S_V$ ,

$$\theta_{iz}^{(U)} = \sum_{i \in S_U} \theta_{iz}^{(U)} \frac{k_{iz}^{(U)}}{\sum_{i \in S_U} k_{iz}^{(U)}}, \quad \theta_{jz}^{(V)} = \sum_{j \in S_V} \theta_{jz}^{(V)} \frac{k_{jz}^{(V)}}{\sum_{j \in S_V} k_{jz}^{(V)}}. \tag{18}$$

The process for generating a mixture network described here can also be used to generate a unipartite, directed network. However, for our bipartite network version, model identifiability problem should be addressed before the model be used for generating random bipartite networks (the solution to parameters is not unique, which is treated in detail in **Appendix B** and discussed in **Discussion**). This problem can be solved easily by introducing an extra constraint  $\sum_i \theta_{iz}^{(U)} = \sum_j \theta_{jz}^{(V)}$ . As a consequence, we have

$$\theta_{iz}^{(U)} = \frac{k_{iz}^{(U)}}{\sqrt{\sum_i k_{iz}^{(U)}}}, \quad \theta_{jz}^{(V)} = \frac{k_{jz}^{(V)}}{\sqrt{\sum_j k_{jz}^{(V)}}}. \tag{19}$$

The details are available in **Appendix B**.

## B. Simulation results

We use three indices to measure the performance of the algorithm in this subsection: the fraction of correctly classified vertices, the Jaccard index for

*overlapping vertices* (vertices belonging to more than one module), and variant normalized mutual information (NMI) [35]. Since our algorithm allows one vertex to belong to multiple modules, a node is correctly classified if the predicted memberships for all modules are correct. The definition of the Jaccard index is as follows: let  $S_1$  denote the known set of overlapping vertices, and  $S_2$  is the predicted set of overlapping vertices; the Jaccard index is defined as  $|S_1 \cap S_2| / |S_1 \cup S_2|$ . NMI measures the similarity between actual community structures and predictions from the view of information theory: it is 1 if the prediction is exactly the same as the actual condition, and is 0 when they are independent. If a generated random network has any isolated nodes, they would be removed from the network before detecting the modules, and so cannot be used to measure the performance of the algorithm.

The total number of vertices is fixed to 2000 for all networks in our consistency tests. For random unipartite networks, adjacency matrices of  $2000 \times 2000$  are generated. For random bipartite networks, adjacency matrices of  $1000 \times 1000$  are generated, so that the total number of vertices is unchanged. For mixture networks, adjacency matrices of  $1500 \times 1500$  are generated with 1000 common vertices (50%), the total number of unique vertices is still 2000.

To begin with, we perform three consistency tests on random networks with 2 modules. In the first sets of consistency testing, 55% of vertices belong to module 1, 55% to module 2 (10% to both modules). The total expected number of links of each vertex is set to be  $k$ . Detailedly, if a node is a specific vertex that only belongs to one module, its expected number of linkage to this module is  $k$ ; on the other hand, if a specific vertex belongs to two modules, its expected number of linkage to both modules are  $k/2$ . For a common vertex, the numbers of linkages for it in both vertex sets are set to be  $k/2$  if it belongs to only one module and  $k/4$  if it belongs to two modules.

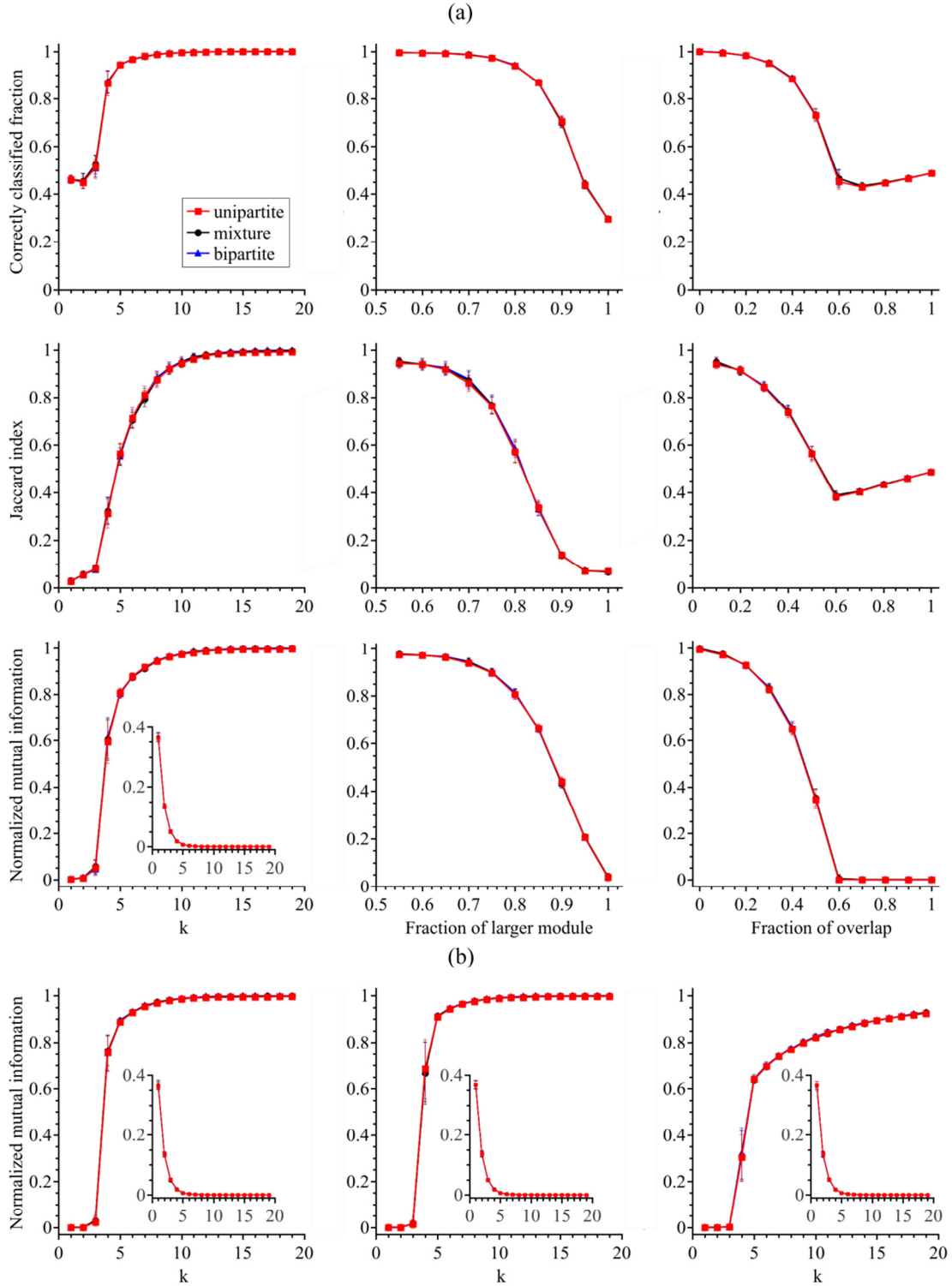


FIG 2. (color online) Results from consistency tests for random networks (a) with 2 modules and (b) with more than 2 modules described in the text. Each point is the average over 50 random networks. For each network, 30 random initializations are used, and the run with the highest log likelihood is chosen as the final result. The insets show the fraction of isolated nodes for networks of each  $k$  for the corresponding



tests. For the second and the third sets of testing of random networks with 2 modules, since  $k$  is fixed at a large value (10), only a few networks occasionally contain isolated node(s) (fractions are close to 0), the effects of which to the measured indices are negligible. Thus, their fractions of isolated nodes are not shown.

We test the performance of the algorithm by varying  $k$ . When  $k$  is small, the actual modular structures of networks are quite hard to find. When  $k$  is large, it is quite easy to reveal the modules of networks. As shown in the left panels of Fig. 2, the performance of the algorithm on all types of network increases with  $k$  as expected. When  $k \leq 3$ , the fractions of correctly classified vertices are far away from 0, but NMIs are quite close to 0, indicating that predictions for networks with low degree are random with respect to the actual community structures. The performance at  $k = 4$  increase rapidly. When  $k \geq 10$ , the algorithm can find out the modular structures for all three types of networks with high performance.

In the second sets of consistency testing,  $k$  is fixed at 10, and the fraction of overlapping vertices remains at 10%, but the fraction of vertices belonging to module 1 is increased. The condition when the fraction of vertices belonging to module 1 is smaller than that belonging to module 2 need not to be discussed, which is equivalent to the condition considered here. As suggested by the middle panels of Fig. 2, all indices decrease with further unbalanced fractions of two modules.

In the third sets of testing,  $k$  is fixed at 10, the fractions of modules 1 and 2 are set to be equal, but the fraction of overlapping vertices increases. The right panels of Fig. 2 indicates that all indices decrease with an increase of the fraction of overlapping vertices ( $\leq 0.6$ ). When the fraction of overlapping vertices is large, the fractions of correctly classified vertices and the Jaccard indices increase, but the NMIs are close to 0, indicating that predictions for networks with large fractions of overlapping vertices are also random with respect to the actual community structures.

In all three sets of testing, the curves of both indices for all three types of networks overlap with each other very well at each point (Fig. 2). It suggests that our algorithm has equal performance for three types of networks generated by same

parameters.

We also perform three consistency tests on random networks of more than 2 modules. In these tests, the total number of vertices is still fixed to 2000, the fraction of overlapping nodes is set to 10%, the fractions of nodes specifically belonging to each module are equal, but  $k$  varies. For the overlapping nodes, the numbers of modules they belong are restricted by an integer interval given by the user. Once the interval is given, we randomly generate the number of modules for each overlapping node and randomly assign it to such number of modules.

To begin with, we set the number of modules to be 5, and each overlapping node belongs to 2 modules. Since that the fraction of correctly classified vertices is hard to calculate for random networks with more than 2 modules, and that the Jaccard index for overlapping vertices cannot reflect whether they are assigned to the correct modules, these two indices are not calculated in the following tests. As shown in the left panel of Fig. 2(b), NMI increases with the increasing  $k$ . Similar results are observed for two sets of random networks with 10 modules, with each overlapping vertex belongs to 2 modules (Fig. 2(b), middle panel) and belongs to 2-10 modules (Fig. 2(b), right panel). For the latter, the curves for all three types of networks increase slower than those of the former.

In sum, results of consistency tests suggest that our algorithm can perform well for a large range of parameters for all three types of networks. All indices increase with increasing  $k$ , and approach 1 for random networks with 2 modules when the difference between the fractions of two modules or the fraction of overlapping vertices is small.

## IV. SIMULATIONS OF SYNTHETIC NETWORKS GENERATED BY SAMPLING

### A. Synthetic networks generated by sampling

Next, we test the performance of the algorithm based on synthetic networks generated by sampling, the pseudocode of which is given in Fig. 3. In this process,  $r$  random unipartite networks are generated for each measured parameter of network quality, and for each random unipartite network, we generate  $s$  networks by sampling.

Note that in sampling, some information is lost, since many elements in the adjacency matrix of the unipartite network become unknown in sampled networks.

```

foreach network quality
  (1) generate  $r$  random unipartite networks;
  foreach random unipartite network
    foreach sampling rule
      (2) sample  $s$  sub-networks;
      (3) find modules;
      (4) calculate prediction measures;
    end
  end
end

```

FIG 3. Pseudocode of generating random networks by sampling.

Random unipartite networks used in this section are generated by two well-known benchmarks: the Girvan-Newman (GN) benchmark [2, 36] and the Lancichinetti-Fortunato-Radicchi (LFR) benchmark [37-39], which are of non-overlapping community. Using algorithms allowing overlapping community to detect non-overlapping community is quite straightforward by assigning nodes to the most probable module. For the GN benchmark, there are 128 vertices and 4 modules in each generated random network, with expected degree 16 for each node. Compared to the GN benchmark, it is more difficult to examine community structure in random networks generated by the LFR benchmark. For the LFR benchmark, we generate random unipartite networks with 1000 nodes, community size ranging from 20 to 100 (labeled “B”), and all other parameters are same as those used in Ref. [39]. Both directed and undirected random networks of two benchmarks are generated using softwares described by Refs. [37-39]. The difficulty of finding network modules are controlled by the mixing parameter  $\mu$ , which determines the ratio of external degree linking to other modules to total degree of a node. When  $\mu$  increases, community structure is more mixed. The community structure vanishes when  $\mu$  is large enough.

We define two sampling rules, symmetric and asymmetric sampling. For *symmetric sampling*, the fractions of specific vertices in  $U$  and  $V$  are the same

(denoted as  $u$  and  $v$ ), with the fraction of common vertices being changed (denoted as  $c$ ). For both benchmarks, we change  $c$  from 0 to 1, which determines the type of synthetic network generated by sampling: (1)  $c=0$ , the sampled networks are bipartite; (2)  $c=1$ , the sampled networks are unipartite and identical to the original unipartite network; (3)  $0 < c < 1$ , the sampled networks are mixture networks. For *asymmetric sampling*, we fix  $c$ , and then change  $u$  and  $v$  accordingly. These three parameters are not independent; their sum is always 1.

## B. Simulation results

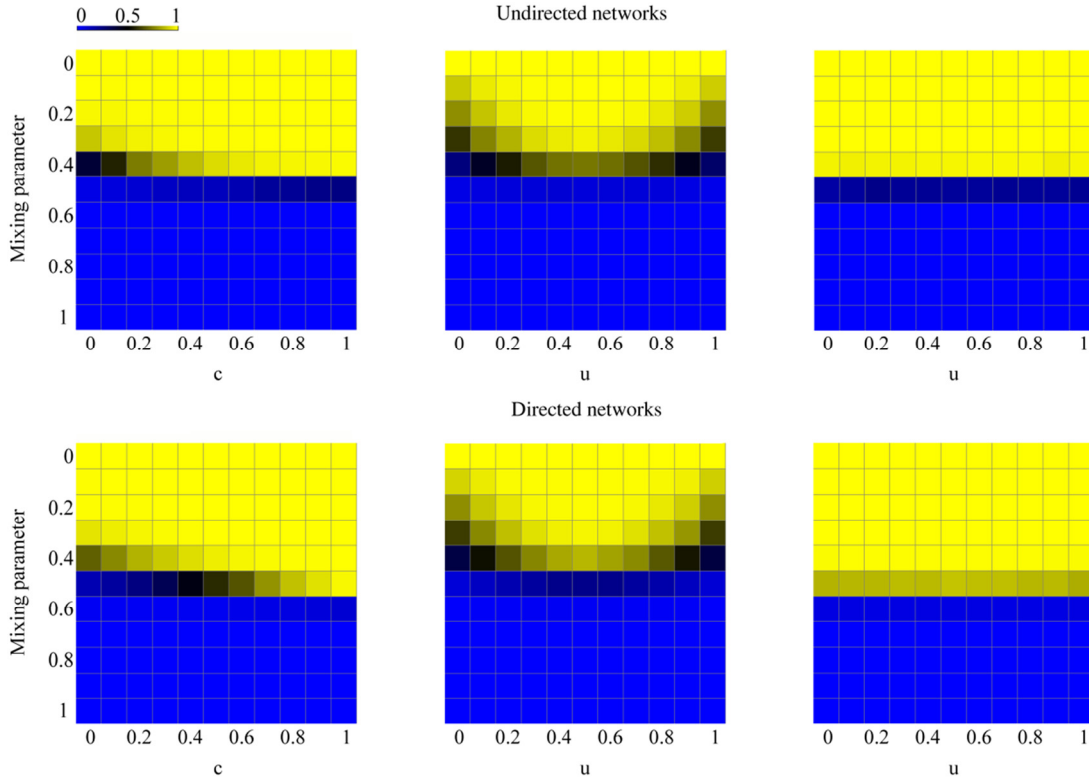


FIG 4. (color online) Heat maps for normalized mutual information of our model on random networks generated by symmetric sampling (left panels), asymmetric sampling with  $c=0.2$  (middle panels), and asymmetric sampling with  $c=0.8$  (right panels) using the GN benchmark (directed and undirected networks), which are created with `matrix2png` [40]. Both  $r$  and  $s$  are set to be 10. Fifty random initializations are used for the module detection of each network.

First, we apply our algorithm to a set of symmetric sampling undirected networks generated from the GN benchmark. As shown in Fig. 4 (left upper panel), when  $\mu$

increases, NMIs decrease for random networks with any  $c$  as expected. When  $\mu \leq 0.3$ , there is no huge difference between the NMIs of networks with different  $c$ . When  $\mu = 0.4$ , the performance for our model on networks with small  $c$  begin to decrease. The smaller  $c$ , the worse the performance. It is not hard to understand, since the fraction of unknown edges increases with the decrease of  $c$ . When  $\mu \geq 0.5$ , the performance vanishes. The tendency for the performance of symmetric sampling for directed networks is generally similar to those of undirected ones, despite the difference in the point of decrease Fig. 4 (left lower panel).

For the GN benchmark, we also apply the algorithm to four sets of asymmetric sampling networks,  $c$  of which are fixed to 0.2 and 0.8 (two tests for undirected networks and two for directed networks). For the former tests, the performance for networks of  $u = 0.5$  decrease most slowly, since they have more remaining known edges than those of other fractions (Fig. 4, middle panels). For the latter test, performances for all  $u$  are quite similar, since  $c = 0.8$ , no matter how  $u$  and  $v$  change, the information loss is quite similar (Fig. 4, right panels).

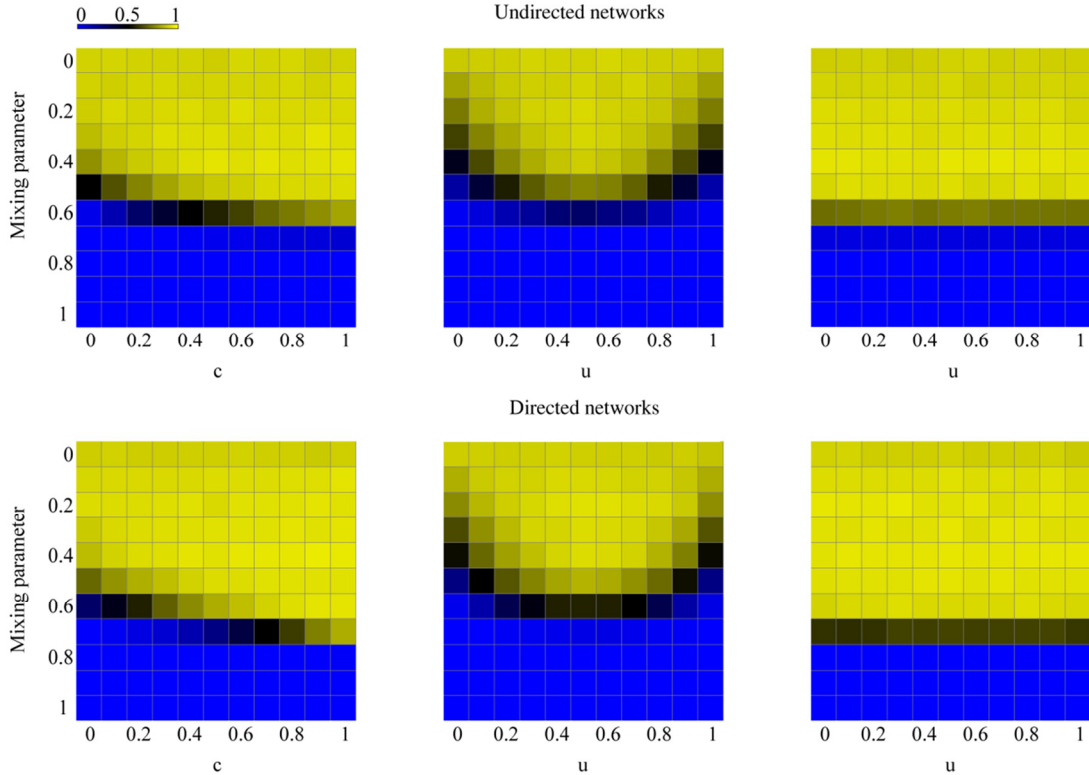


FIG 5. (color online) Heat maps for normalized mutual information of our model on random networks generated by symmetric sampling (left panels), asymmetric sampling with  $c = 0.2$  (middle panels), and asymmetric sampling with  $c = 0.8$  (right panels) using the LFR benchmark (directed and undirected networks), which are created with matrix2png.  $r$  is set to be 10 and  $s$  are set to be 5. Ten random initializations are used for the module detection of each network.

For the LFR benchmark, we also apply our algorithm to two sets of symmetric sampling networks and four sets of asymmetric sampling networks. Similar results are obtained from this harder test compared to these of the GN benchmark. For the symmetric sampling undirected networks (Fig. 5, left upper panel), when  $\mu \leq 0.5$ , the algorithm easily finds the modules, despite that the performance for networks with  $c$  close to 0 begin to decrease when  $\mu$  is close to 0.5. When  $\mu = 0.6$ , the performance decreases. The smaller  $c$ , the worse the performance. When  $\mu \geq 0.7$ , the algorithm fails. For the remaining five tests, the tendency for the performance is also generally similar to those of the GN benchmark, despite the difference in the point of decrease (Fig. 5, left bottom, middle and right panels). The similar tendencies between the performance of our algorithm on the easier and harder tests suggest that our model are applicable not only to small and easy networks but also large and hard ones.

## V. SIMULATIONS OF UNIPARTITE, DIRECTED NETWORKS

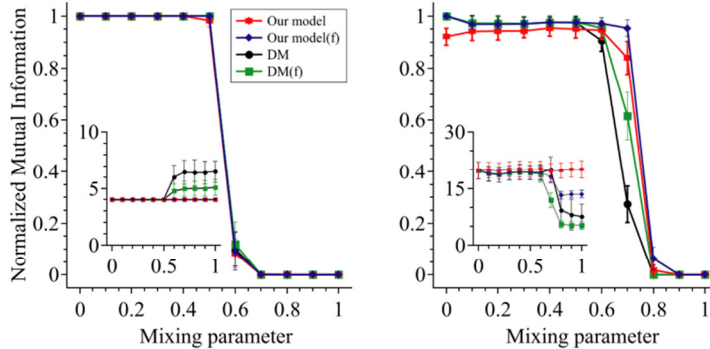


FIG 6. (color online) Performance of the algorithms on random unipartite, directed networks generated using GN (left panel) and LFR benchmarks (right panel). The

optimized algorithms are marked with (f) following their names. Each data point is averaged over 100 networks. The insets show the numbers of modules given to our model (i.e., the actual number of modules) and those found by DM, DM(f) and our model(f). The numbers of random initializations of our model for two panels are 100 and 10, respectively.

In this section, we apply our model on random unipartite, directed networks generated by GN and LFR benchmarks, and compare it with the optimization of a modularity defined in the context of a directed network (denoted as DM) [41]. The optimization process is carried out by the RADATOOLS software [42] using extremal optimization [43].

The data shown in Fig. 6 indicate that our model has similar performance with DM on random unipartite, directed networks generated using GN and LFR benchmarks. The numbers of modules found by DM tend to depart from the actual number when  $\mu$  is large for both benchmarks (Fig. 6, insets).

We further optimize the results of DM and our model using a combinatorial optimization strategy of fast algorithm [44] and reposition algorithm by the RADATOOLS software. For the GN benchmark, the performances for optimized algorithms are similar to those of unoptimized algorithms (Fig. 6, left panel). On the other hand, the performances for algorithms increase after optimization for the LFR benchmark (Fig. 6, right panel).

## VI. SIMULATIONS OF BIPARTITE NETWORKS

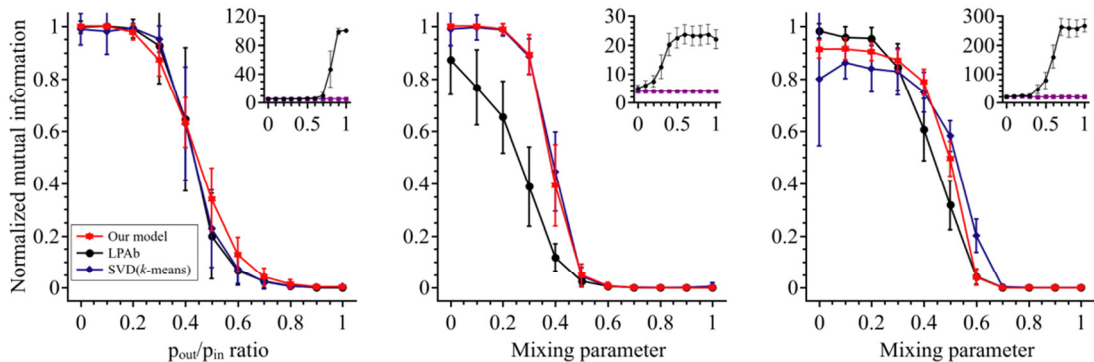


FIG 7. (color online) Performance of the algorithms on random bipartite networks

generated following Ref. [9] averaged over 100 networks for each data point (left panel), generated by symmetric sampling from the GN benchmark (middle panel,  $m=10$ ,  $n=10$ ), or generated by symmetric sampling from the LFR benchmark (right panel,  $m=10$ ,  $n=5$ ). The insets show the actual number of modules (violet solid line, rectangle) and those found by LPAb (black solid line, ellipse). For SVD( $k$ -means) and our model, the numbers of modules are given. The numbers of random initializations of our model for three panels are 100, 50 and 10, respectively.

Next, we apply our algorithm to a set of randomly-generated bipartite networks, following Ref. [9]. Each random bipartite network contains 100 vertices, and consists of 5 modules. In each module, there are 12 vertices in  $U$  and 8 vertices in  $V$ . The difficulty of predicting is controlled by the ratio  $p_{out}/p_{in}$ , where  $p_{out}$  denotes the probability of vertices being connected between different modules and  $p_{in}$  refers to the probability of vertices being linked within the same module. Links only exist between vertices in  $U$  and those in  $V$ .

We compare our algorithm with LPAb [11] and a spectral algorithm based on singular value decomposition [12], two state-of-the-art algorithms that can find community structure in bipartite networks. LPAb is based on a label-propagation algorithm (LPA) [45], which assigns unique labels to nodes and repeatedly updates the label of each vertex by assigning the most frequent labels of its neighbors until it meets the terminal condition. Barber and Clark [11] reformulated LPA as an optimization problem, addressed its drawback with additional constraints, and produced several variant LPA algorithms. LPAb is one of the variants that can be used to find modules in bipartite networks. LPA and its variants can determine the number of modules by themselves.

For bipartite networks, the above-mentioned spectral algorithm finds the modules in three stages: (1) matrix factorization of the adjacency matrix using singular value decomposition; (2) dimensionality reduction using  $k$ -rank least-squares approximation; and (3) clustering vertices in the reduced space. In the third step,



various clustering methods can be used, including the  $k$ -means clustering algorithm and the cosine matrix reordering mentioned in Ref. [12]. Here we used  $k$ -means for the spectral algorithm, denoted as SVD( $k$ -means).

The data shown in the left panel of Fig. 7 suggests that all three algorithms have similar performance in this set of tests (100 node-randomly generated bipartite networks). Notably, when  $p_{out}/p_{in}$  is small, LPAb gives the correct number of modules; when  $p_{out}/p_{in}$  is large, it gives a very large number of modules (Fig. 7, the inset in the left panel).

We also compare our algorithm with LPAb and SVD( $k$ -means) on bipartite networks generated by symmetric sampling. For bipartite networks sampled from the GN benchmark, our algorithm and SVD( $k$ -means) perform better than LPAb when  $\mu \leq 0.4$  (Fig. 7, middle panel). A possible explanation for why the performance of LPAb is less good in this data set is that the numbers of modules given by LPAb depart from the the correct number even when  $\mu$  is small (Fig. 7, the inset in the middle panel). For bipartite networks sampled from the LFR benchmark, all three algorithms have similar performance (Fig. 7, right panel). An exception is for SVD( $k$ -means) at  $\mu = 0.0$ . At this point, SVD( $k$ -means) performs poorly and has a larger standard derivation. This phenomenon is caused by  $k$ -means clustering rather than singular value decomposition, since replacing  $k$ -means with hierarchical clustering [46] as clustering method for the spectral algorithm can achieve good performance ( $NMI = 1 \pm 0$ ) at  $\mu = 0.0$ .

In total, the comparison of three models indicate that the performance of our model, when used for detecting non-overlapping communities for bipartite networks, is competitive with LPAb and SVD( $k$ -means).

## VII. REAL NETWORKS

### A. Southern women bipartite network

We apply our algorithm to a well-known real-world bipartite network, the southern women dataset [47], which consists of 18 women (W1-W18) and 14 social

events (E1-E14). This dataset has been studied extensively to investigate the results of various methods [48].

To make the result comparable to other algorithms, first we display the result of our algorithm by assigning nodes to two non-overlapping modules. The non-overlapping partition divides the 18 women into W1-W9 and W10-W18, which agrees with the “perfect” partition as suggested in Ref. [48] (Fig. 8, upper panel). Unlike many algorithms mentioned in Ref. [48], our algorithm also assigns social events to modules along with women. For the social events, E1-E8 belong to the same module with W1-W9, and E9-E14 with W10-W18.

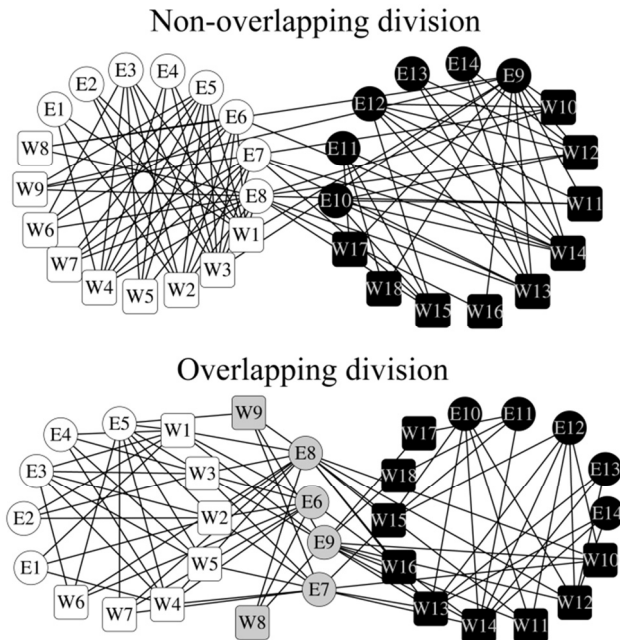


FIG 8. (color online) Non-overlapping (upper panel) and overlapping division (lower panel) of the bipartite southern women network. Network visualization is created with Cytoscape [49]. Nodes colored with black or white belong to only one module, and those colored with gray belong to both modules simultaneously.

When allowing overlapping modules, W8 and W9, and E6-E9 belong to both modules (Fig. 8, lower panel). This is quite reasonable, since all links only exist between those overlapping nodes and the remaining specific nodes of two modules. In another words, these overlapping nodes maintain the connection between these two modules.

## B. Transcriptional regulatory mixture network

Next, we apply our algorithm to a recently-released human transcriptional regulatory network [50] obtained from Ref. [15], which is a mixture, directed network. This dataset consists of 82 transcriptional factors (TFs) and 3998 downstream target genes, which include 31 TFs. The number of modules is set at 30. One hundred random initializations are used for the algorithm and the run with the highest log likelihood is chosen as final result. For 30 modules, the average number of TFs is 5.3, and the average number of target genes is 242.2.

Modular structures found in the network can find genes known to be related or offer new biological insights. The underlying assumption is that genes in the same module tend to be involved in the same or similar biological pathways. Gene ontology (GO) [51] is a standard tool that can be used to associate biological functions with gene sets. Here, we perform GO enrichment analysis [52] to determine the enriched GO terms for downstream target genes. We report two case studies on the modules found in this transcriptional regulatory network. Supplementary Fig. 1 displays a module consisting of 3 TFs and 469 downstream target genes (including 2 TFs). The enriched GO terms are mainly related to the cell cycle and the metabolic process (supplementary Table I). There are three TFs here: *HDAC2*, *NFKB1*, and *NFYA*. All three genes are known to be related to the cell cycle [53-56], and *NFYA* is related to the metabolic process[57].

A second case study focuses on a module related to the immune system (supplementary Fig. 2). It consists 130 downstream genes (including 2 TFs) and 10 TFs, 6 of which (*IRF1*, *POLR3A*, *POU2F2*, *PRDMI*, *FOSL2*, and *IRF4*) are related to the immune system [58-62]. For downstream genes, the enriched GO terms are shown in supplementary Table II, many of which are immune-related. We predict that another 4 TFs (*PBX3*, *POU5F1*, *PPARGCIA*, and *MAFK*) may also be related to the immune system.

## VIII. DISCUSSION

In this paper, we present a probabilistic method for identifying community structures in unipartite, bipartite, and mixture networks in a unified framework. Our

model can assign vertices to one module, multiple modules, or none of the modules. When the network is bipartite or mixture, it can simultaneously assign memberships to both sets of nodes.

We test the performance of our algorithm by applying it to several sets of synthetic networks (both overlapping and non-overlapping communities) and two real-world networks. Our model can perform well on large parameter ranges in synthetic networks, and are applicable to real-world networks. For the southern women bipartite dataset, our model offers reasonable overlapping and non-overlapping community divisions. For the human transcriptional regulatory network (a mixture, directed network), modules associated with biological functions are reported in two case studies, which can reveal related genes or provide new clues. Preliminary analysis for mixture, undirected networks (two genetic interaction networks built from epistatic mini-array profiles) also confirm the ability of our algorithm to find modules with biological significance [63]. Along with the simulation and real network results of BKN (unipartite, undirected network version) mentioned in Ref. [6] on unipartite, undirected networks, we conclude that our algorithm performs well on all three types of network, and is competitive with other algorithms for unipartite and bipartite networks.

The main contributions of our model are: (1) It introduces the concept of the mixture network, which can represent a wild range of networks that are neither unipartite nor bipartite in many fields including biology and social science, and can operate on this type of data. To our knowledge, this is the first network community detection algorithm to focus this question; (2) It offers a unified framework for unipartite, bipartite and mixture networks; and (3) This framework can potentially be used for the generalization of other community detection algorithms focusing on the unipartite network and maybe other models in the fields of complex network.

One may note that, for bipartite network version model, the solution for  $\theta_{iz}^{(U)}$  and  $\theta_{jz}^{(V)}$  is not unique even for the same local maxima, that is, it suffers from the problem of model identifiability. For any solution, multiplying a positive constant  $C$  for all

$\theta^{(U)}$  and dividing the same constant for all  $\theta^{(V)}$  is still a solution to the model. However, since the product of  $\theta_{iz}^{(U)}$  and  $\theta_{jz}^{(V)}$  remain unchanged, which does not affect the value of  $q_{ij}(z)$ , the quantity that we are concerned with, we can ignore this problem when the algorithm is used to detect network modules. However, when the method is used to generate random bipartite networks (Sec. III), a constraint for parameters is needed as shown in **Appendix B**. The model identifiability problem does not exist when the network is unipartite or mixture.

Similar to Ref. [6], the main drawback of this algorithm is that it is unable to determine the number of module  $K$  from the data. Methods for model selection, such as the Akaike information criterion [64], the Bayesian information criterion [65], or the likelihood ratio test [66], are not applicable here, the reason for which is the same as that in Ref. [6], i.e., that many parameters are zero violates the assumption of model selection methods.

We also note that in real-world data, edges are sometimes associated with weights or scores that can be used to indicate the reliability of the links [15, 19, 21]. We are planning to address this issue combined with the problem of determining the number of modules in future based on the current framework.

## ACKNOWLEDGEMENTS

The authors gratefully thank Junwei Wang for useful and detailed discussions on the statistical techniques related to the model and careful reading of the manuscript, Illes Farkas, Minghua Deng, and Lin Wang for comments and suggestions, Iain Bruce for detailed proof reading of the manuscript, Jun Wang for checking the mathematical parts, and Lingli Jiang for her epistatic mini-array profile experiments, as the motivation of this model was generated while analyzing her data.

## APPENDIX A: SOLUTION OF MIXTURE NETWORK VERSION MODEL

The likelihood function and constraint are given by Eq. (11) and (12). Taking the logarithm of Eq. (11) and introducing an arbitrary variable  $q_{ij}(z)$  that satisfies  $\sum_z q_{ij}(z) = 1$ , we have

$$\ln P(G | \theta^{(U)}, \theta^{(V)}) \geq \sum_{ijz} \left[ A_{ij} q_{ij}(z) \ln \left( \frac{\theta_{iz}^{(U)} \theta_{jz}^{(V)}}{q_{ij}(z)} \right) - \theta_{iz}^{(U)} \theta_{jz}^{(V)} \right]. \quad (\text{A1})$$

Now we consider the constraint in Eq. (12). Let  $L$  denote the target function, which is given by

$$L = \sum_{ijz} \left[ A_{ij} q_{ij}(z) \ln \left( \frac{\theta_{iz}^{(U)} \theta_{jz}^{(V)}}{q_{ij}(z)} \right) - \theta_{iz}^{(U)} \theta_{jz}^{(V)} \right] + \sum_{ijz} c_{ijz} \delta_{i^{(U)}, j^{(V)}} \left( \theta_{iz}^{(U)} - \theta_{jz}^{(V)} \right), \quad (\text{A2})$$

where  $c_{ijz}$  is the Lagrange multiplier. Differentiating Eq. (A2) with respect to  $\theta_{iz}^{(U)}$  leads to

$$\begin{aligned} \frac{\partial L}{\partial \theta_{iz}^{(U)}} &= \sum_j \left[ \frac{A_{ij} q_{ij}(z)}{\theta_{iz}^{(U)}} - \theta_{jz}^{(V)} + c_{ijz} \delta_{i^{(U)}, j^{(V)}} \right] \\ &= \frac{\sum_j A_{ij} q_{ij}(z)}{\theta_{iz}^{(U)}} - \sum_j \theta_{jz}^{(V)} + \sum_j c_{ijz} \delta_{i^{(U)}, j^{(V)}} \\ &= 0. \end{aligned} \quad (\text{A3})$$

As a consequence,

$$\theta_{iz}^{(U)} = \frac{\sum_j A_{ij} q_{ij}(z)}{\sum_j \theta_{jz}^{(V)} - \sum_j c_{ijz} \delta_{i^{(U)}, j^{(V)}}}. \quad (\text{A4})$$

Similarly, we have

$$\theta_{jz}^{(V)} = \frac{\sum_i A_{ij} q_{ij}(z)}{\sum_i \theta_{iz}^{(U)} + \sum_i c_{ijz} \delta_{i^{(U)}, j^{(V)}}}. \quad (\text{A5})$$

We shall only consider the condition for common vertices, since for other vertices, Eq. (A4) and (A5) become Eq. (10). For each pair of common vertices  $i'$  and  $j'$  that  $\delta_{i'^{(U)}, j'^{(V)}} = 1$ . Inserting Eqs. (A4) and (A5) to Eq. (12), we can get

$$c_{i'j'} = \frac{-\sum_i \theta_{iz}^{(U)} \sum_j A_{ij} q_{ij}(z) + \sum_j \theta_{jz}^{(V)} \sum_i A_{ij} q_{ij}(z)}{\sum_i A_{ij} q_{ij}(z) + \sum_j A_{ij} q_{ij}(z)} \quad \forall z. \quad (\text{A6})$$

Inserting Eq. (A6) into (A4),

$$\begin{aligned}
\theta_{iz}^{(U)} &= \frac{\sum_j A_{ij} q_{ij}(z) \sum_i A_{ij} q_{ij}(z) + \left( \sum_j A_{ij} q_{ij}(z) \right)^2}{\sum_j \theta_{jz}^{(V)} \sum_j A_{ij} q_{ij}(z) + \sum_i \theta_{iz}^{(U)} \sum_j A_{ij} q_{ij}(z)} \\
&= \frac{\sum_i A_{ij} q_{ij}(z) + \sum_j A_{ij} q_{ij}(z)}{\sum_j \theta_{jz}^{(V)} + \sum_i \theta_{iz}^{(U)}}.
\end{aligned} \tag{A7}$$

Similarly, by inserting Eq. (A6) into (A5), we have

$$\theta_{jz}^{(V)} = \frac{\sum_i A_{ij} q_{ij}(z) + \sum_j A_{ij} q_{ij}(z)}{\sum_i \theta_{iz}^{(U)} + \sum_j \theta_{jz}^{(V)}}. \tag{A8}$$

## APPENDIX B. GENERATING RANDOM NETWORKS

We start from Eq. (14). By multiplying the denominator of the right side at both sides of the first equation, and summing over all common vertices, we have

$$\sum_{j \in O_V} \theta_{jz}^{(V)} \sum_i \theta_{iz}^{(U)} + \sum_{i \in O_U} \theta_{iz}^{(U)} \sum_j \theta_{jz}^{(V)} = \sum_{i \in O_U} k_{iz}^{(U)} + \sum_{j \in O_V} k_{jz}^{(V)}. \tag{B1}$$

Similarly, starting from Eq. (15), we get

$$\begin{aligned}
\sum_{i \in S_U} \theta_{iz}^{(U)} \sum_j \theta_{jz}^{(V)} &= \sum_{i \in S_U} k_{iz}^{(U)}, \\
\sum_{j \in S_V} \theta_{jz}^{(V)} \sum_i \theta_{iz}^{(U)} &= \sum_{j \in S_V} k_{jz}^{(V)}.
\end{aligned} \tag{B2}$$

The goal here is to find out the solutions for  $\theta^{(U)}$  and  $\theta^{(V)}$ , given that each  $k_{iz}^{(U)}$  and  $k_{jz}^{(V)}$  is known. To make symbols simpler, we define  $X = \sum_{i \in S_U} \theta_{iz}^{(U)}$ ,

$Y = \sum_{i \in O_U} \theta_{iz}^{(U)}$ ,  $Z = \sum_{j \in S_V} \theta_{jz}^{(V)}$ , and  $W = \sum_{j \in O_V} \theta_{jz}^{(V)}$ , so that,

$$X + Y = \sum_i \theta_{iz}^{(U)}, \quad Z + W = \sum_j \theta_{jz}^{(V)}, \tag{B3}$$

and  $\alpha = \sum_{i \in S_U} k_{iz}^{(U)}$ ,  $\beta = \sum_{i \in O_U} k_{iz}^{(U)}$ ,  $\gamma = \sum_{j \in S_V} k_{jz}^{(V)}$ , and  $\zeta = \sum_{j \in O_V} k_{jz}^{(V)}$ , so that

$$\alpha + \beta = \sum_i k_{iz}^{(U)}, \quad \gamma + \zeta = \sum_j k_{jz}^{(V)}. \tag{B4}$$

Eqs. (B1) and (B2) can be rewritten as

$$W(X + Y) + Y(Z + W) = \beta + \zeta, \tag{B5}$$

$$X(Z + W) = \alpha, \tag{B6}$$

$$Z(X + Y) = \gamma. \tag{B7}$$

Solving the equations using  $Y = W$ , we can get

$$X = \frac{2\alpha}{\gamma - \alpha + \beta + \zeta} Y, \quad (\text{B8})$$

$$Z = \frac{2\gamma}{\alpha - \gamma + \beta + \zeta} Y. \quad (\text{B9})$$

Inserting Eq. (B8) and (B9) into Eq. (B6), we get

$$\therefore Y = \sqrt{\frac{(\beta + \zeta)^2 - (\alpha - \gamma)^2}{2(\alpha + \gamma + \beta + \zeta)}}. \quad (\text{B10})$$

Now the values of  $\sum_{i \in O_U} \theta_{iz}^{(U)}$ ,  $\sum_{i \in S_U} \theta_{iz}^{(U)}$ ,  $c$ , and  $\sum_{j \in O_V} \theta_{jz}^{(V)}$  can be given by

$$\begin{aligned} \sum_{i \in O_U} \theta_{iz}^{(U)} &= \sqrt{\frac{\left(\sum_{i \in O_U} k_{iz}^{(U)} + \sum_{j \in O_V} k_{jz}^{(V)}\right)^2 - \left(\sum_{i \in S_U} k_{iz}^{(U)} - \sum_{j \in S_V} k_{jz}^{(V)}\right)^2}{2\left(\sum_{i \in S_U} k_{iz}^{(U)} + \sum_{j \in S_V} k_{jz}^{(V)} + \sum_{i \in O_U} k_{iz}^{(U)} + \sum_{j \in O_V} k_{jz}^{(V)}\right)}}, \\ \sum_{i \in S_U} \theta_{iz}^{(U)} &= \frac{2\sum_{i \in S_U} k_{iz}^{(U)}}{\sum_{j \in S_V} k_{jz}^{(V)} - \sum_{i \in S_U} k_{iz}^{(U)} + \sum_{i \in O_U} k_{iz}^{(U)} + \sum_{j \in O_V} k_{jz}^{(V)}} \sum_{i \in O_U} \theta_{iz}^{(U)}, \\ \sum_{j \in S_V} \theta_{jz}^{(V)} &= \frac{2\sum_{j \in S_V} k_{jz}^{(V)}}{\sum_{i \in S_U} k_{iz}^{(U)} - \sum_{j \in S_V} k_{jz}^{(V)} + \sum_{i \in O_U} k_{iz}^{(U)} + \sum_{j \in O_V} k_{jz}^{(V)}} \sum_{i \in O_U} \theta_{iz}^{(U)}, \\ \sum_{j \in O_V} \theta_{jz}^{(V)} &= \sum_{i \in O_U} \theta_{iz}^{(U)}. \end{aligned} \quad (\text{B11})$$

For common vertices, start from Eq. (14), we have

$$\sum_i \theta_{iz}^{(U)} + \sum_j \theta_{jz}^{(V)} = \frac{\sum_{i \in O_U} k_{iz}^{(U)} + \sum_{j \in O_V} k_{jz}^{(V)}}{\sum_{i \in O_U} \theta_{iz}^{(U)}}. \quad (\text{B12})$$

Inserting back to Eq. (14), we have

$$\begin{aligned} \theta_{iz}^{(U)} &= \sum_{i \in O_U} \theta_{iz}^{(U)} \frac{k_{iz}^{(U)} + k_{jz}^{(V)}}{\sum_{i \in O_U} k_{iz}^{(U)} + \sum_{j \in O_V} k_{jz}^{(V)}}, \\ \theta_{jz}^{(V)} &= \sum_{j \in O_V} \theta_{jz}^{(V)} \frac{k_{iz}^{(U)} + k_{jz}^{(V)}}{\sum_{i \in O_U} k_{iz}^{(U)} + \sum_{j \in O_V} k_{jz}^{(V)}}. \end{aligned} \quad (\text{B13})$$

Similarly, for specific nodes, we have

$$\theta_{iz}^{(U)} = \sum_{i \in S_U} \theta_{iz}^{(U)} \frac{k_{iz}^{(U)}}{\sum_{i \in S_U} k_{iz}^{(U)}}, \quad \theta_{jz}^{(V)} = \sum_{j \in S_V} \theta_{jz}^{(V)} \frac{k_{jz}^{(V)}}{\sum_{j \in S_V} k_{jz}^{(V)}}. \quad (\text{B14})$$

Next we will show this solution is agreed with that of BKN in the context of a unipartite, undirected network. For such a network,  $\alpha = 0$ ,  $\gamma = 0$ ,  $\beta = \zeta$ , as a



consequence,  $X = 0$ ,  $Z = 0$ , and

$$\begin{aligned}
Y &= \sqrt{\frac{(\beta + \zeta)^2}{2(\beta + \zeta)}} \\
&= \sqrt{\frac{\beta + \zeta}{2}} \\
&= \sqrt{\beta} \\
&= \sqrt{\sum_{i \in O_U} k_{iz}^{(U)}},
\end{aligned} \tag{B15}$$

which is exactly same as Eq. (7) in [6].

On the other side, for bipartite networks we have  $\beta = 0$  and  $\zeta = 0$  and therefore  $\alpha = \gamma$ . Since the bipartite network version model suffers from model identifiability problem, we can introduce an extra constraint  $X = Z$  to solve the problem, and get  $X = Z = \sqrt{\alpha}$ . As a consequence,

$$\theta_{iz}^{(U)} = \frac{k_{iz}^{(U)}}{\sqrt{\sum_i k_{iz}^{(U)}}}, \quad \theta_{iz}^{(U)} = \frac{k_{iz}^{(U)}}{\sqrt{\sum_i k_{iz}^{(U)}}}. \tag{B16}$$

## References

- [1] S. Fortunato, *Phy. Rep.* **486**, 75 (2010).
- [2] M. E. J. Newman, and M. Girvan, *Phys. Rev. E* **69**, 026113 (2004).
- [3] G. Palla, I. Derenyi, I. Farkas, and T. Vicsek, *Nature (London)* **435**, 814 (2005).
- [4] M. E. J. Newman, and E. A. Leicht, *Proc. Natl. Acad. Sci. USA* **104**, 9564 (2007).
- [5] J. M. Hofman, and C. H. Wiggins, *Phys. Rev. Lett.* **100**, 258701 (2008).
- [6] B. Ball, B. Karrer, and M. E. J. Newman, *Phys. Rev. E* **84**, 036103 (2011).
- [7] B. Karrer, and M. E. J. Newman, *Phys. Rev. E* **83**, 016107 (2011).
- [8] R. Guimera, M. Sales-Pardo, and L. A. Amaral, *Phys. Rev. E* **76**, 036102 (2007).
- [9] M. J. Barber, *Phys. Rev. E* **76**, 066102 (2007).
- [10] S. Lehmann, M. Schwartz, and L. K. Hansen, *Phys. Rev. E* **78**, 016108 (2008).
- [11] M. J. Barber, and J. W. Clark, *Phys. Rev. E* **80**, 026129 (2009).
- [12] S. Sarkar, and A. Dong, *Phys. Rev. E* **83**, 046114 (2011).
- [13] M. E. J. Newman, *Nat. Phys.* **8**, 25 (2012).
- [14] T. I. Lee *et al.*, *Science* **298**, 799 (2002).
- [15] M. B. Gerstein *et al.*, *Nature (London)* **489**, 91 (2012).
- [16] H. Salgado *et al.*, *Nucleic Acids Res.* **41**, D203 (2013).
- [17] H. Dinkel, C. Chica, A. Via, C. M. Gould, L. J. Jensen, T. J. Gibson, and F. Diella, *Nucleic Acids Res.* **39**, D261 (2011).
- [18] J. B. Glattfelder, and S. Battiston, *Phys. Rev. E* **80**, 036104 (2009).
- [19] M. Costanzo *et al.*, *Science* **327**, 425 (2010).
- [20] A. Frost *et al.*, *Cell* **149**, 1339 (2012).
- [21] C. J. Ryan *et al.*, *Mol. Cell* **46**, 691 (2012).
- [22] L. L. Jiang *et al.* (manuscript in preparation).
- [23] M. Schuldiner, S. R. Collins, N. J. Thompson, V. Denic, A. Bhamidipati, T. Punna, J. Ihmels, B. Andrews, C. Boone, and J. F. Greenblatt, *Cell* **123**, 507 (2005).
- [24] D. Fiedler *et al.*, *Cell* **136**, 952 (2009).
- [25] A. Vinayagam, U. Stelzl, R. Foulle, S. Plassmann, M. Zenkner, J. Timm, H. E. Assmus, M. A. Andrade-Navarro, and E. E. Wanker, *Sci. Signal.* **4**, rs8 (2011).
- [26] J. Bellay *et al.*, *Genome Res.* **21**, 1375 (2011).
- [27] T. Zhou, J. Ren, M. Medo, and Y. C. Zhang, *Phys. Rev. E* **76**, 046115 (2007).
- [28] C. Ryan, D. Greene, A. Guérolé, H. van Attikum, N. J. Krogan, P. Cunningham, and G. Cagney, *BMC Syst. Biol.* **5**, 80 (2011).
- [29] X.-L. Meng, and D. B. Rubin, *Biometrika* **80**, 267 (1993).
- [30] R. M. Neal, and G. E. Hinton, in *Learning in Graphical Models* (Springer, 1998), pp. 355.
- [31] In Ball *et al.*, this criterion is defined using strict inequality. However, in our implementation, the equal condition (or nearly equal) is also considered. Suppose there is a node with only one link, which belongs to module  $z$  with weight very close to 1, it is reasonable to assign this node to module  $z$ .
- [32] A. Costa, and P. Hansen, *Phys. Rev. E* **84**, 058101 (2011).
- [33] We also propose a model specific for a mixture, undirected network in the supplementary information. However, we could not see any significant difference between the specific model and the model mentioned in the main text from simulation results.
- [34] A. Allard, P. A. Noel, L. J. Dube, and B. Pourbohloul, *Phys. Rev. E* **79**, 036113 (2009).

- [35] A. Lancichinetti, S. Fortunato, and J. Kertész, *New J. Phys.* **11**, 033015 (2009).
- [36] M. Girvan, and M. E. J. Newman, *Proc. Natl. Acad. Sci. USA* **99**, 7821 (2002).
- [37] A. Lancichinetti, S. Fortunato, and F. Radicchi, *Phys. Rev. E* **78**, 046110 (2008).
- [38] A. Lancichinetti, and S. Fortunato, *Phys. Rev. E* **80**, 016118 (2009).
- [39] A. Lancichinetti, and S. Fortunato, *Phys. Rev. E* **80**, 056117 (2009).
- [40] P. Pavlidis, and W. S. Noble, *Bioinformatics* **19**, 295 (2003).
- [41] A. Arenas, J. Duch, A. Fernández, and S. Gómez, *New J. Phys.* **9**, 176 (2007).
- [42] <http://deim.urv.cat/~sgomez/radatools.php>
- [43] J. Duch, and A. Arenas, *Phys. Rev. E* **72**, 027104 (2005).
- [44] M. E. J. Newman, *Phys. Rev. E* **69**, 066133 (2004).
- [45] U. N. Raghavan, R. Albert, and S. Kumara, *Phys. Rev. E* **76**, 036106 (2007).
- [46] A. R. Martinez, and W. L. Martinez, Naval Surface Warfare Center, Dahlgren Division, Tech. Rep (2004).
- [47] A. Davis, B. B. Gardner, and M. R. Gardner, *Deep South* (The University of Chicago Press, Chicago, 1941).
- [48] L. C. Freeman, in *Dynamic social network modeling and analysis* (The National Academies Press, Washington, 2003), pp. 39.
- [49] P. Shannon, A. Markiel, O. Ozier, N. S. Baliga, J. T. Wang, D. Ramage, N. Amin, B. Schwikowski, and T. Ideker, *Genome Res.* **13**, 2498 (2003).
- [50] This dataset is known as "enets7.K562\_proximal\_filtered\_network.txt", which is detailedly described in the supplementary information of Gerstein et al.
- [51] M. Ashburner *et al.*, *Nat. Genet.* **25**, 25 (2000).
- [52] E. I. Boyle, S. Weng, J. Gollub, H. Jin, D. Botstein, J. M. Cherry, and G. Sherlock, *Bioinformatics* **20**, 3710 (2004).
- [53] N. D. Perkins, L. K. Felzien, J. C. Betts, K. Leung, D. H. Beach, and G. J. Nabel, *Science* **275**, 523 (1997).
- [54] J. Kucharczak, M. J. Simmons, Y. Fan, and C. Gelinas, *Oncogene* **22**, 8961 (2003).
- [55] I. Manni, G. Caretti, S. Artuso, A. Gurtner, V. Emiliozzi, A. Sacchi, R. Mantovani, and G. Piaggio, *Mol. Biol. Cell* **19**, 5203 (2008).
- [56] K. H. Jung *et al.*, *J. Cell Biochem.* **113**, 2167 (2012).
- [57] S. D. Clarke, *J. Nutr.* **131**, 1129 (2001).
- [58] A. Lehtonen, R. Lund, R. Lahesmaa, I. Julkunen, T. Sareneva, and S. Matikainen, *Cytokine* **24**, 81 (2003).
- [59] M. N. Lee *et al.*, *Nat. Immunol.* **14**, 179 (2013).
- [60] L. M. Corcoran, M. Karvelas, G. J. Nossal, Z. S. Ye, T. Jacks, and D. Baltimore, *Genes. Dev.* **7**, 570 (1993).
- [61] G. Cattoretti, C. Angelin-Duclos, R. Shakhovich, H. Zhou, D. Wang, and B. Alobeid, *J. Pathol.* **206**, 76 (2005).
- [62] V. C. Foletta, D. H. Segal, and D. R. Cohen, *J. Leukoc. Biol.* **63**, 139 (1998).
- [63] C. Chang *et al.* (manuscript in preparation).
- [64] H. Akaike, *IEEE Trans. Autom. Control* **19**, 716 (1974).
- [65] G. Schwarz, *Ann. Stat.* **6**, 461 (1978).
- [66] J. A. Rice, *Mathematical Statistics and Data Analysis* (Duxbury Press, 1995).